He, M., & Macdonald, J. H. G. (2016). An analytical solution for the galloping stability of a 3 degree-of-freedom system based on quasisteady theory. Journal of Fluids and Structures, 60, 23-36. DOI: 10.1016/j.jfluidstructs.2015.10.004

Journal of Fluids and Structures 60 (2016) 23–36

Contents lists available at ScienceDirect

Journal of Fluids and Structures

journal homepage: www.elsevier.com/locate/jfs

An analytical solution for the galloping stability of a 3 degree-of-freedom system based on quasi-steady theory

Mingzhe He *, John H.G. Macdonald

Department of Civil Engineering, University of Bristol, Bristol BS8 1TR, UK

ARTICLE INFO

Article history:
Received 12 January 2015
Accepted 12 October 2015

Keywords:
3DOF galloping
Eigenvalue problem
Stability
Quasi-steady theory

ABSTRACT

The aerodynamic forces on a two-dimensional three-degree-of-freedom (3DOF-heave, sway and torsion) body of arbitrary cross-section are considered, for arbitrary wind direction relative to the principal structural axes. The full 3DOF aerodynamic damping matrix is derived, based on quasi-steady theory, using the commonly-used concept of an aerodynamic centre to represent the effect of the torsional velocity on the aerodynamic forces. The aerodynamic coefficients are assumed to be consistent functions of only the relative angle of attack. It is shown that the determinant of the quasi-steady aerodynamic damping matrix is always zero. The galloping stability of the aerodynamically coupled system is then addressed by formulating the eigenvalue problem, for which analytical solutions are derived for the case of perfectly tuned structural natural frequencies. The solutions define a non-dimensional effective aerodynamic damping coefficient, indicating how stable the system is. A trivial solution always exists, with zero effective aerodynamic damping, corresponding to rotation about the aerodynamic centre, and relatively simple exact closed-form solutions are derived for the other one or two solutions, the minimum solution defining the stability of the system. Example results are presented and discussed for square, rectangular (aspect ratio 3) and equilateral triangular sections and a lightly iced cable, and they are compared with results using previous solutions for 2DOF translational and 1DOF pure torsional galloping. For the shapes considered it is found that the stability of the 3DOF system is normally close to that of the 2DOF translational system, with a relatively small influence of the stability of the torsional degree of freedom, although in some instances, especially at the critical angles of attack, it can significantly affect the stability.

1. Introduction

Galloping instability of slender structures has been widely observed in practice, especially for electricity transmission lines, bridge cable stays, etc.. There has been long lasting interest in predicting such dynamic instability by using aerodynamic coefficients in theoretical models, based on quasi-steady theory. The Den Hartog (1932) criterion provides a prediction of galloping instability but is limited to single-degree-of-freedom (1DOF) motion normal to the wind direction, which is not always the case in practice. Aerodynamic coupling between degrees of freedom can be important, especially when the structural natural frequencies are close to each other.

* Corresponding author. Tel.: +44 117 331 5726.
E-mail addresses: mingzhe.he@bristol.ac.uk (M. He), john.macdonald@bristol.ac.uk (J.H.G. Macdonald).

http://dx.doi.org/10.1016/j.jfluidstructs.2015.10.004
0889-9746/

It is well known that for long span bridges, aircraft wings, etc., flutter instability, i.e. an aeroelastic instability involving torsional motion, is a major concern. Often this is treated as a two-degree-of-freedom (2DOF) problem, involving vertical and torsional motion. For the analysis of flutter of real structures normally numerical approaches are used but Chen and Kareem (2006) proposed a closed-form solution of coupled vertical and torsional flutter for long span bridges, based on flutter derivatives, showing good agreement with experimental results. It should be pointed out that for bridge decks the reduced velocity is quite low resulting in low accuracy of quasi-steady theory. Therefore, flutter derivatives (or equivalent) are commonly used instead. But for smaller diameter bodies, especially cables, the reduced velocity is generally high so quasi-steady theory, as used in conventional Den Hartog galloping, is more applicable, since the timescale of oscillations is much longer than the timescale for the flow to pass the body. In these conditions, as in the present paper which considers a generalisation of quasi-steady theory, 'galloping' is potentially a more appropriate term than 'flutter'.

There is quite a long history of analysing coupled vertical and torsional motions using quasi-steady theory, often called two-degree-of-freedom galloping and often achieving good agreement with experiment results (Blevins and Iwan, 1974, Modi and Slater, 1983, Novak, 1969, Slater, 1969), as reviewed by Blevins (1994). Related to this, Norberg (1993) conducted a series of experiments on rectangular prisms, allowing not only translational motions but also torsion. These were followed up with numerical simulations (Sohankar et al., 1997) which focused on the flow around the cross-section at 0° incidence and the effects of the aspect ratio of the rectangular section, giving some insight into the underlying flow mechanisms driving the instability. Robertson et al. (2003) also performed numerical simulations on rectangular prisms with various side ratios, addressing both the onset of galloping and the steady-state amplitudes of the resulting vibrations. Although the study was conducted at low Reynolds numbers, good agreement was achieved between the numerical results and quasi-steady theory.

Jones (1992) was the first to address coupled translational galloping (across-wind and along-wind), for the special case of perfectly tuned natural frequencies in the two directions. Li et al. (1998) also proposed a series of equations for 2DOF coupled translational galloping, but using body co-ordinates to allow inclination of the wind, which lost the direct connection to the Den Hartog criterion. These and other developments in the analysis of coupled 2DOF translational galloping have recently been critically reviewed by Nikitas and Macdonald (2014). Another useful recent review of various issues in galloping is provided by Piccardo et al. (2014a)

The Den Hartog criterion was generalised to allow for the effects of Reynolds number and any orientation of the cylinder and the plane of 1DOF motion by Macdonald and Larose (2006), for application to dry inclined galloping of bridge stay-cables. The approach was then extended to address the onset of galloping instability of a generalised coupled translational 2DOF model (Macdonald and Larose, 2008a,b), providing a closed-form solution for the minimum structural damping required to prevent galloping in the case of perfectly tuned natural frequencies, and numerical solutions and limit cases for detuned natural frequencies. Meanwhile Carassale et al. (2005) developed an equivalent formulation expressing the aerodynamic damping matrix in terms of vectors and matrix calculus, but excluding Reynolds number effects. These analyses were able to reproduce some of features of dry inclined cable galloping observed in dynamic wind tunnel tests. Also, Luongo and Piccardo (2005) presented an approximate analytical solution for coupled translational galloping, using a perturbation method, which was found to be valid not only in the quasi-resonant condition but also the non-resonant one. Later Piccardo et al. (2011) further investigated the critical conditions for 2DOF translational galloping and explicitly presented the aerodynamic damping matrix of such a system considering both the angle of attack and yaw angle.

There has been a limited amount of research on coupled three-degree-of-freedom (3DOF) galloping. Yu et al. (1993a,b) extended Jones (1992) work by including the torsional degree of freedom, deriving the governing equations using a perturbation approach and solving them for the onset of galloping using the Routh–Hurwitz method. Wang and Lilien (1998) also proposed a 3DOF model, allowing for both single and bundled transmission lines, which was solved using time history simulations. However, both of these 3DOF models focused on the eccentricity and full span effects rather than the aerodynamic coupling between the degrees of freedom and a simplified definition of the conditions for the galloping to occur. Later Luongo et al. (2007), using a linear curved-beam model to analyse galloping, suggested, from order-of-magnitude considerations, that the torsional velocity has negligible influence on the aerodynamic forces. More recently Gjelstrup and Georgakis (2011) developed a 3DOF model based on the 2DOF translational model by Macdonald and Larose (2008a,b) but incorporating torsion. They allowed for variations in Reynolds number and skew angle, as well as angle of attack, which may be relevant in some situations but complicate the formulation considerably. Their solution of the galloping problem was based on the Routh–Hurwitz criterion, which defines whether or not the system is stable but requires significant numerical calculations to quantify the stability. In other developments, Piccardo (1993) addressed coupled aeroelastic phenomena generally and presented the two-dimensional 3DOF quasi-steady aerodynamic damping matrix for certain conditions. Recently, he and his co-workers re-visited the problem and presented the matrix in a more general form (Piccardo et al., 2014a). They have also considered the aeroelastic behaviour of slender tower structures using quasi-steady theory, specifically addressing the dynamic behaviour of the whole structure and nonlinear effects, and presenting some numerical results for the stability Piccardo et al. (2014b). As far as the authors are aware these references cover virtually all the previous analysis of 3DOF galloping.

The aim of the current paper is to address the 3DOF galloping problem, focussing on obtaining a closed-form solution for the effective aerodynamic damping of the system for the first time, albeit for the simplified system of a two-dimensional body with perfectly tuned natural frequencies in the three structural modes. Such a system may be particularly relevant to bundled conductors, which have close natural frequencies for both torsional and translational motions (Chabart and Lilien,

1998), and it acts as a reference case for other more involved multi-degree-of-freedom galloping situations. The analysis is based on the recent work by Nikitas and Macdonald (2014) on generalisation of the Den Hartog galloping criterion for coupled translational galloping. They derived the aerodynamic damping matrix of the two-dimensional translational 2DOF model, for arbitrary orientation of the principal structural axes, by Taylor expansion for small motion, and discussed the different stability criteria that apply in different conditions for the 1DOF and 2DOF systems. In this paper, a similar approach is applied to obtain the aerodynamic damping matrix of the two-dimensional 3DOF model, including torsion, then an exact analytical solution is found for the stability of the aerodynamically coupled system for the case of perfect tuning and example results are presented and discussed.

2. Derivation of the 3DOF aerodynamic damping matrix

The proposed 3DOF model aims to identify the galloping stability of a body of arbitrary rigid cross-section, considered in two dimensions. Fig. 1 shows the geometry of the system, using a lightly iced cable as an example. In the proposed approach herein, inertial coupling is not considered, so the elastic centre (point O) coincides with the centre of mass. This is valid for symmetrical sections and for lightly iced sections where the shift in the centre of mass due to the ice is negligible. The rotational velocity of the cross-section can be important but there is no rigorous theoretical way of dealing with it in a quasi-steady manner for bluff bodies. Therefore, the common approach of the use of an aerodynamic centre is applied, which was first adopted by Slater (1969) from flutter analysis of aerofoils (Theodorsen, 1935) and later systematically explained by Blevins (1994). The aerodynamic forces on the body are taken to be the same as those on the body if stationary and subject to a wind velocity equal to the relative velocity between the wind and the aerodynamic centre (point A), which includes a component due to the rotational velocity of the body about point O.

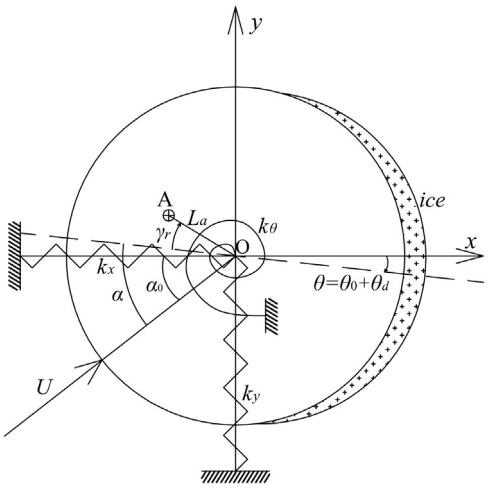

Fig. 1. 3DOF cross-sectional model.

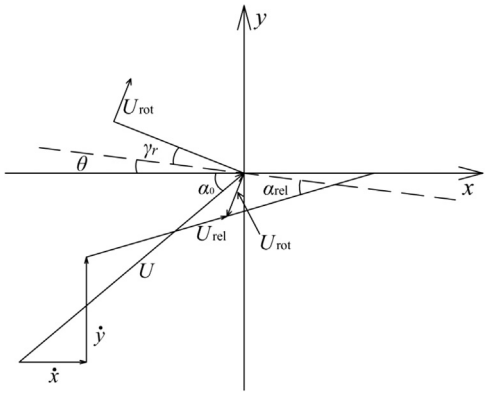

Fig. 2. Mean wind velocity, components of velocity of the aerodynamic centre, and hence relative velocity between the wind and aerodynamic centre.

In Fig. 1 the x and y directions are the principal structural axes of the system and θ is the rotation of the cross-section, measured between the x axis and a reference line on the body (the dashed line in Fig. 1 fixed to the cross-sectional shape). θ includes the static rotation of the shape, θ_0 (e.g. due to the weight of ice accretion or the mean wind load), and a dynamic component, θ_d. k_x, k_y and k_θ represent the structural stiffnesses, which can be expressed as $m\omega_x^2$, $m\omega_y^2$ and $J_\theta\omega_\theta^2$, respectively. m is the mass per unit length of the body and $J_\theta = mr^2$ is the polar mass moment of inertia per unit length about point O, where r is the radius of gyration. ω_x, ω_y and ω_θ are the angular natural frequencies of the uncoupled structural system in each degree of freedom. The aerodynamic centre is positioned at radius L_a from O at an angle γ_r from the body reference line. α_0 is the angle between the wind direction and the x axis, while α represents the angle between the wind direction and the body reference line ($\alpha = \alpha_0 + \theta$).

Fig. 2 shows the velocities of the wind and the body. U is the mean wind velocity, at an angle of α_0 with respect to the x axis. $\dot{x}$ and $\dot{y}$ are the components of the translational velocity of the body in the x and y directions. $U_{\text{rot}} = L_a\dot{\theta}$ is the component of velocity of the aerodynamic centre due to the rotational velocity of the section. The relative velocity, U_{rel}, is then the resultant of all the above velocity components. The corresponding relative angle of attack is denoted as α_{rel}. Hence, based on the quasi-steady assumption, the aerodynamic forces in the x and y directions (F_x and F_y respectively) and moment about O (F_θ) on the body per unit length are given by

$$F_x = \frac{1}{2}\rho {U_{\text{rel}}}^2 D\left(-C_L(\alpha_{\text{rel}})\sin(\alpha_{\text{rel}}-\theta) + C_D(\alpha_{\text{rel}})\cos(\alpha_{\text{rel}}-\theta)\right), \tag{1}$$

$$F_y = \frac{1}{2}\rho {U_{\text{rel}}}^2 D\left(C_L(\alpha_{\text{rel}})\cos(\alpha_{rel}-\theta) + C_D(\alpha_{\text{rel}})\sin(\alpha_{rel}-\theta)\right), \tag{2}$$

$$F_\theta = \frac{1}{2}\rho {U_{\text{rel}}}^2 D^2 C_M(\alpha_{\text{rel}}), \tag{3}$$

where ρ is the density of air, D is a reference dimension of the body and $C_D(\alpha)$, $C_L(\alpha)$ and $C_M(\alpha)$ are, respectively, the static drag, lift and moment coefficients of the cross-section, which are taken to be only functions of the angle of attack, α.

The magnitude of the instantaneous relative wind velocity and the relative angle of attack are given by

$$U_{\text{rel}} = \sqrt{\left(U\sin\ \alpha_0 - \dot{y} - \dot{\theta}L_a\cos(\gamma_r+\theta)\right)^2 + \left(U\cos\ \alpha_0 - \dot{x} - \dot{\theta}L_a\sin(\gamma_r+\theta)\right)^2}, \tag{4}$$

$$\alpha_{\text{rel}} = \arctan\left(\frac{U\sin\ \alpha_0 - \dot{y} - \dot{\theta}L_a\cos(\gamma_r+\theta)}{U\cos\ \alpha_0 - \dot{x} - \dot{\theta}L_a\sin(\gamma_r+\theta)}\right) + \theta. \tag{5}$$

To consider the onset of galloping instability, Taylor expansion about the static values is applied to the aerodynamic forces and moment and only the linear terms in the velocity components of the body are retained

$$F_x = F_x|_{\dot{x}=\dot{y}=\dot{\theta}=\theta_d=0} + \dot{x}\left.\frac{\partial F_x}{\partial \dot{x}}\right|_{\dot{x}=\dot{y}=\dot{\theta}=\theta_d=0} + \dot{y}\left.\frac{\partial F_x}{\partial \dot{y}}\right|_{\dot{x}=\dot{y}=\dot{\theta}=\theta_d=0} + \dot{\theta}\left.\frac{\partial F_x}{\partial \dot{\theta}}\right|_{\dot{x}=\dot{y}=\dot{\theta}=\theta_d=0}, \tag{6}$$

$$F_y = F_y|_{\dot{x}=\dot{y}=\dot{\theta}=\theta_d=0} + \dot{x}\left.\frac{\partial F_y}{\partial \dot{x}}\right|_{\dot{x}=\dot{y}=\dot{\theta}=\theta_d=0} + \dot{y}\left.\frac{\partial F_y}{\partial \dot{y}}\right|_{\dot{x}=\dot{y}=\dot{\theta}=\theta_d=0} + \dot{\theta}\left.\frac{\partial F_y}{\partial \dot{\theta}}\right|_{\dot{x}=\dot{y}=\dot{\theta}=\theta_d=0}, \tag{7}$$

$$F_\theta = F_\theta|_{\dot{x}=\dot{y}=\dot{\theta}=\theta_d=0} + \dot{x}\left.\frac{\partial F_\theta}{\partial \dot{x}}\right|_{\dot{x}=\dot{y}=\dot{\theta}=\theta_d=0} + \dot{y}\left.\frac{\partial F_\theta}{\partial \dot{y}}\right|_{\dot{x}=\dot{y}=\dot{\theta}=\theta_d=0} + \dot{\theta}\left.\frac{\partial F_\theta}{\partial \dot{\theta}}\right|_{\dot{x}=\dot{y}=\dot{\theta}=\theta_d=0}, \tag{8}$$

In order to evaluate the derivatives, the chain rule is used

$$\frac{d()}{d\dot{x}} = \frac{\partial()}{\partial U_{\text{rel}}}\frac{dU_{\text{rel}}}{d\dot{x}} + \frac{\partial()}{\partial \alpha_{\text{rel}}}\frac{d\alpha_{\text{rel}}}{d\dot{x}} \tag{9}$$

and similarly for $\dot{y}$ and $\dot{\theta}$.

Hence, the full aerodynamic damping matrix for the 3DOF model is derived:

$$\mathbf{C_a} = -\left[\begin{matrix} \frac{\partial F_x}{\partial \dot{x}} & \frac{\partial F_x}{\partial \dot{y}} & \frac{\partial F_x}{\partial \dot{\theta}} \\ \frac{\partial F_y}{\partial \dot{x}} & \frac{\partial F_y}{\partial \dot{y}} & \frac{\partial F_y}{\partial \dot{\theta}} \\ \frac{\partial F_\theta}{\partial \dot{x}} & \frac{\partial F_\theta}{\partial \dot{y}} & \frac{\partial F_\theta}{\partial \dot{\theta}} \end{matrix}\right]_{\dot{x}=\dot{y}=\dot{\theta}=\theta_d=0}, \tag{10}$$

which is found to be

$$\mathbf{C_a} = \frac{\rho D U}{2}\begin{bmatrix} 2C_D & 2C_L & (C_L'+C_D) & (C_L-C_D') & 0 & 0 \\ 2C_L & -2C_D & (C_L-C_D') & -(C_L'+C_D) & 0 & 0 \\ 0 & 0 & 0 & 0 & 2DC_M & DC_M' \end{bmatrix}\begin{bmatrix} c^2 & cs & L_a s_{\alpha\theta\gamma} c \\ -cs & -s^2 & -L_a s_{\alpha\theta\gamma} s \\ s^2 & -cs & -L_a c_{\alpha\theta\gamma} s \\ cs & -c^2 & -L_a c_{\alpha\theta\gamma} c \\ c & s & L_a s_{\alpha\theta\gamma} \\ -s & c & L_a c_{\alpha\theta\gamma} \end{bmatrix}, \tag{11}$$

where $c = \cos\alpha_0$, $s = \sin\alpha_0$, $c_{\alpha\theta\gamma} = \cos(\alpha_0+\theta_0+\gamma_r)$, $s_{\alpha\theta\gamma} = \sin(\alpha_0+\theta_0+\gamma_r)$ and primes indicate derivatives with respect to angle of attack.

It should be noted that the aerodynamic coefficients and their derivatives should be evaluated at the angle between the wind and the shape in the static equilibrium configuration about which the dynamic stability is considered, i.e. at $\alpha_0+\theta_0$ ($=\alpha$ for $\theta_d=0$).

Eq. (11) is a generalised version of the aerodynamic damping matrix proposed by Piccardo (1993), allowing not only for arbitrary orientation of the principal axes but also for arbitrary location of the aerodynamic centre. The top left 2×2 sub-matrix of $\mathbf{C_a}$ is identical to the aerodynamic damping matrix for 2DOF translational galloping presented by Nikitas and Macdonald (2014) or a simplified version of the ones given by Strømmen and Hjorth-Hansen (1995), Macdonald and Larose (2008a) and Piccardo et al. (2011), who all allowed for a skew angle in the third dimension. The other elements of $\mathbf{C_a}$ are found to agree with the equivalent equations given by Gjelstrup and Georgakis (2011) (except for an apparent transcription error for their $\frac{\partial F_y}{\partial \theta}$), after substitution of certain angle variables and neglecting the terms allowing for the differentials with respect to Reynolds number and skew angle.

An interesting finding about the 3DOF quasi-steady aerodynamic damping matrix is that its determinant is always zero. This is not generally true for any pair of two DOFs. The reason is that the velocity of the aerodynamic centre due to the rotational velocity of the section can be decomposed into components in the x and y directions, so its effect is equal to a linear combination of the translational velocities in those directions. Therefore the third column of the aerodynamic damping matrix, which relates to the torsional velocity, is a linear combination of the other two columns ($L_a s_{\theta\gamma}$ times the first column plus $L_a c_{\theta\gamma}$ times the second column, where $s_{\theta\gamma} = \sin(\theta_0+\gamma_r)$ and $c_{\theta\gamma} = \cos(\theta_0+\gamma_r)$). It is well known that such a matrix has a determinant of zero.

For the special case of $\alpha_0 = 0$, i.e. the wind direction along the x axis, the aerodynamic damping matrix simplifies to

$$\mathbf{C_a} = \frac{\rho D U}{2}\begin{bmatrix} 2C_D & -(C_L-C_D') & L_a\left[2C_D s_{\theta\gamma} - \left(C_L-C_D'\right)c_{\theta\gamma}\right] \\ 2C_L & (C_L'+C_D) & L_a\left[2C_L s_{\theta\gamma} + \left(C_L'+C_D\right)c_{\theta\gamma}\right] \\ 2DC_M & DC_M' & DL_a\left[2C_M s_{\theta\gamma} + C_M' c_{\theta\gamma}\right] \end{bmatrix}, \tag{12}$$

which agrees with the 3DOF aerodynamic damping matrix given by Piccardo et al. (2014a) if also $\theta_0 = 0$.

It should be mentioned that aerodynamic stiffness terms (see e.g. Piccardo et al., 2014a) are excluded in the present analysis to focus on the effects of the aerodynamic damping matrix, which is normally dominant in determining the stability of dynamic responses. For wide cross-sections large negative aerodynamic stiffness can cause static divergence, but for compact cross-sections, i.e. with low width to depth ratios, normally the aerodynamic stiffness only has a minor effect. This is because for such cross-sections it is small relative to the structural stiffness, whilst the aerodynamic damping terms are comparable to the structural damping terms (Gjelstrup and Georgakis, 2011). Furthermore, including only the aerodynamic damping matrix, an exact analytical solution for the galloping stability can be found, as shown in the following section, which can act as a reference case even when the aerodynamic stiffness may have some influence.

3. Analytical solution for the galloping stability of a 3DOF perfectly tuned system

In order to obtain the galloping stability criterion of the 3DOF system its eigenvalue problem is now studied. The matrix equation of motion of the system, after subtracting the static components and neglecting any inertial coupling or aerodynamic stiffness, is given by:

$$\mathbf{M}\ddot{\mathbf{X}} + \mathbf{C_s}\dot{\mathbf{X}} + \mathbf{K}\mathbf{X} = -\mathbf{C_a}\dot{\mathbf{X}} \tag{13}$$

where dots indicate derivatives with respect to time and

$$\mathbf{M} = \begin{bmatrix} m & 0 & 0 \\ 0 & m & 0 \\ 0 & 0 & J_\theta \end{bmatrix},\ \mathbf{C_s} = \begin{bmatrix} 2m\omega_x\zeta_x & 0 & 0 \\ 0 & 2m\omega_y\zeta_y & 0 \\ 0 & 0 & 2J_\theta\omega_\theta\zeta_\theta \end{bmatrix},\ \mathbf{K} = \begin{bmatrix} m\omega_x^2 & 0 & 0 \\ 0 & m\omega_y^2 & 0 \\ 0 & 0 & J_\theta\omega_\theta^2 \end{bmatrix},\ \mathbf{X} = \begin{Bmatrix} x \\ y \\ \theta_d \end{Bmatrix},$$

where ζ_x, ζ_y and ζ_θ are the structural damping ratios for each degree of freedom.

The total damping matrix $\mathbf{C}$ is the sum of the aerodynamic damping matrix and the structural damping matrix:

$$\mathbf{C}=\begin{bmatrix} c_{xx} & c_{xy} & c_{x\theta} \\ c_{yx} & c_{yy} & c_{y\theta} \\ c_{\theta x} & c_{\theta y} & c_{\theta\theta} \end{bmatrix}=\mathbf{C_a}+\mathbf{C_s}. \tag{14}$$

Since $\mathbf{C}$ is asymmetric, the eigenvalues are generally complex. A widely used way of solving such an eigenvalue problem is to express it in space-state matrix form, with

$$\mathbf{A}=\begin{bmatrix} \mathbf{0} & \mathbf{I} \\ -\mathbf{M^{-1}K} & -\mathbf{M^{-1}C} \end{bmatrix}, \tag{15}$$

where $\mathbf{I}$ is the identity matrix. The characteristic polynomial is then given by

$$|\mathbf{A}-\lambda\mathbf{I}|=0. \tag{16}$$

This is a 6th order polynomial in the eigenvalues, λ, the solutions of which are either real or complex conjugate pairs. Conventionally, the eigenvalues and eigenvectors are found numerically, but this gives limited insight into the behaviour. In this paper, in contrast, an analytical solution is obtained, for the galloping stability of a perfectly tuned 3DOF system. Clearly this is a special case which would rarely occur in practice, but for some tension structures such as bundled conductors the natural frequencies can be very close to each other (Chabart and Lilien, 1998), so it is not unreasonable to consider this condition. Also it acts as a reference case in which the effects of the aerodynamic damping coupling between the structural modes are maximised, since any forcing on one degree of freedom due to unforced motion of another occurs at its natural frequency. In contrast, for well detuned modes the coupling is unimportant and the behaviour tends towards that of uncoupled degrees of freedom or the 2DOF systems previously considered.

For the perfectly tuned system all the uncoupled structural angular natural frequencies, ω_x, ω_y and ω_θ are set equal to ω_n. Following the approach taken by Macdonald and Larose (2008a), solutions are sought on the stability boundary, so there is a pair of eigenvalues with zero real part, $\lambda=\pm\mathbf{i}\omega$ (or a single eigenvalue with $\omega=0$), where ω is the angular natural frequency of the coupled self-excited motion. The characteristic polynomial can then be separated into real and imaginary parts. The imaginary part can be rearranged as

$$b_1Z^2-b_2Z-b_2\omega_n^2=0 \tag{17}$$

and the real part can be expressed as

$$Z(Z^2-b_3Z-b_3\omega_n^2)=0, \tag{18}$$

where $Z=\omega^2-\omega_n^2$ and b_1, b_2 and b_3 are given by

$$b_1=\frac{(c_{xx}+c_{yy})J_\theta+mc_{\theta\theta}}{mJ_\theta}, \tag{19}$$

$$b_2=\frac{|\mathbf{C}|}{m^2J_\theta}, \tag{20}$$

$$b_3=\frac{m\left(c_{\theta\theta}c_{xx}+c_{\theta\theta}c_{yy}-c_{x\theta}c_{\theta x}-c_{y\theta}c_{\theta y}\right)+J_\theta(c_{xx}c_{yy}-c_{xy}c_{yx})}{m^2J_\theta}. \tag{21}$$

Note that these equations apply for any damping matrix.

3.1. First condition for galloping

It is obvious that $Z=0$ is a solution of Eq. (18), which by the definition of Z leads to $\omega=\omega_n$. Since Eq. (17) must also be satisfied, this leads to $b_2=0$. Hence, from the definition of b_2, the determinant of the total damping matrix $|\mathbf{C}|$ must equal zero. This is a general condition for any damping matrix of a 3DOF system with all three structural natural frequencies being identical.

It is convenient to express the aerodynamic damping matrix in the form

$$\mathbf{C_a}=\frac{\rho DU}{2}\begin{bmatrix} 1 & 0 & 0 \\ 0 & 1 & 0 \\ 0 & 0 & r \end{bmatrix}\mathbf{S_a}\begin{bmatrix} 1 & 0 & 0 \\ 0 & 1 & 0 \\ 0 & 0 & r \end{bmatrix}, \tag{22}$$

where $\mathbf{S_a}$ is a non-dimensional matrix, which for the quasi-steady aerodynamic damping matrix in Eq. (11) is given by

$$\mathbf{S_a}=\begin{bmatrix} S_{xx} & S_{xy} & S_{x\theta} \\ S_{yx} & S_{yy} & S_{y\theta} \\ S_{\theta x} & S_{\theta y} & S_{\theta\theta} \end{bmatrix}=\begin{bmatrix} 2C_D & 2C_L & (C_L'+C_D) & (C_L-C_D') & 0 & 0 \\ 2C_L & -2C_D & (C_L-C_D') & -(C_L'+C_D) & 0 & 0 \\ 0 & 0 & 0 & 0 & 2\kappa C_M & \kappa C_M' \end{bmatrix}\begin{bmatrix} c^2 & cs & \varepsilon s_{\alpha\theta\gamma}\, c \\ -cs & -s^2 & -\varepsilon s_{\alpha\theta\gamma}\, s \\ s^2 & -cs & -\varepsilon c_{\alpha\theta\gamma}\, s \\ cs & -c^2 & -\varepsilon c_{\alpha\theta\gamma}\, c \\ c & s & \varepsilon s_{\alpha\theta\gamma} \\ -s & c & \varepsilon c_{\alpha\theta\gamma} \end{bmatrix}, \tag{23}$$

where $\kappa=\frac{D}{r}$ and $\varepsilon=\frac{L_a}{r}$.

The condition that $|\mathbf{C}|=0$ can then be expressed as

$$S_{3D}^3-GS_{3D}^2+HS_{3D}-|\mathbf{S_a}|=0, \tag{24}$$

where

$$G=S_{xx}+S_{yy}+S_{\theta\theta},$$

$$H=S_{xx}S_{\theta\theta}-S_{x\theta}S_{\theta x}+S_{\theta\theta}S_{yy}-S_{\theta y}S_{y\theta}+S_{yy}S_{xx}-S_{yx}S_{xy}$$

and the non-dimensional effective aerodynamic damping coefficient, S_{3D}, is defined as

$$S_{3D}=\frac{4m\omega_n\zeta_a}{\rho DU}, \tag{25}$$

where $\zeta_a=-\zeta_x=-\zeta_y=-\zeta_\theta$ on the stability boundary.

Clearly this can be used to obtain either the critical structural damping to prevent galloping for a given wind speed or the minimum wind speed at which galloping would occur for given structural damping.

It should be noted that Eq. (24) applies for any aerodynamic damping matrix, even if quasi-steady theory does not hold. However, for the quasi-steady aerodynamic damping matrix derived in Section 2 (Eq. (11)), $|\mathbf{C_a}|=|\mathbf{S_a}|=0$, so $S_{3D}=0$ is a solution of Eq. (24). Hence for no structural damping, one of the modes of the aeroelastically coupled system is on the stability boundary. This is discussed further in Section 3.3. Clearly any positive structural damping will stabilise that mode. The other two solutions of Eq. (24) give the instability criterion for the perfectly tuned 3DOF system:

$$S_{3D}=\frac{1}{2}\left(G\pm\sqrt{G^2-4H}\right)<0, \tag{26}$$

Clearly the negative square root gives the more critical solution.

Expressing Eq. (26) in terms of the aerodynamic coefficients it becomes

$$S_{3D}=\frac{1}{2}\Big\{3C_D+C_L'+\kappa\varepsilon\left(2C_Ms_{\alpha\theta\gamma}+C_M'c_{\alpha\theta\gamma}\right) \pm\sqrt{\left(C_D-C_L'-\kappa\varepsilon\left(2C_Ms_{\alpha\theta\gamma}+C_M'c_{\alpha\theta\gamma}\right)\right)^2+8\kappa\varepsilon\left((C_D-C_L')C_M+C_LC_M'\right)s_{\alpha\theta\gamma}+8\left(C_L+\kappa\varepsilon C_Mc_{\alpha\theta\gamma}\right)\left(C_D'-C_L\right)}\Big\}. \tag{27}$$

3.2. Second condition for galloping

There is also another case where Z does not have to be zero. In this case, the quadratic factor in Eq. (18) must be zero, while Eq. (17) still has to be satisfied. Since the solutions of the two quadratic equations must be the same, this leads to the relation $b_3=b_2/\,b_1$. Solving the quadratic equation for Z, ω^2 is then given by

$$\omega^2=\omega_n^2+\frac{1}{2}\left(b_3\pm\sqrt{b_3^2+4b_3\omega_n^2}\right), \tag{28}$$

while the relation $b_3=b_2/\,b_1$ yields

$$8S_{3D}^3-8GS_{3D}^2+2\left(G^2+H\right)S_{3D}-(GH-|\mathbf{S_a}|)=0. \tag{29}$$

Again this applies for any aerodynamic damping matrix. It should be noted that when Eq. (24) has only one real root, we refer to Eq. (29) which has only one real root as well. It is also interesting to notice that in a general sense, i.e., not limited to the quasi-steady theory, the only real root of Eq. (29) equals to the identical real parts of the two complex roots of Eq. (24), the proof of which is given in Appendix A.

Therefore, after applying the quasi-steady theory, $|\mathbf{S_a}|=0$. Hence, $S_{3D}=0$ is always a solution of Eq. (24), with the other two given by Eq. (26). When Eq. (26) does not give real solutions, i.e. when $G^2-4H<0$, there is only one other real root

given by Eq. (29), which equals to the real part of Eq. (26). Thus, in this case, the only non-trivial real solution yields:

$$S_{3D} = \frac{1}{2}G < 0. \tag{30}$$

Hence it is convenient that Eq. (26) (or Eq. (27)) alone covers all possible solutions (apart from the trivial one, $S_{3D} = 0$), using the full expression if it is real or the real part only if it is complex. The two different cases described here resemble the solutions for the perfectly tuned translational 2DOF system (Macdonald and Larose, 2008ab, Piccardo et al., 2011, Nikitas and Macdonald, 2014), for which the normal solution yields $\omega = \omega_n$ and requires the determinant of the total damping matrix to be zero, but there is another possible situation in which ω is not constrained to be ω_n and there are elliptical trajectories in two modes at different frequencies, giving a so-called complex response, first identified by Jones (1992).

3.3. Eigenvectors of the galloping solutions

It is also of interest to identify the eigenvectors, which define the relative amplitudes of the motion in the three degrees of freedom, which may shed light on the physical galloping responses. For the trivial solution, $S_{3D} = 0$, the eigenvector of the solution can be shown to be

$$\left\{ -L_a s_{\theta\gamma}, -L_a c_{\theta\gamma}, 1 \right\}^{\mathrm{T}}.$$

This corresponds to rotation about the aerodynamic centre. There is hence no translational velocity of the centre itself, so, based on the assumptions made, there is no change in the aerodynamic forces due to the motion so there is no resulting aerodynamic damping. This physically explains why $S_{3D} = 0$ is always a solution.

As to the assumptions of the aerodynamic centre, they have rigorous origins for aerofoil flutter analysis (Theodorsen, 1935), for which it is at a point on the chord one-quarters of the way from the leading to the trailing edge. The method is still widely used for aerofoils. It was adopted for the galloping of bluff bodies by Slater (1969) and has since been widely used by many researchers in this field (e.g. Blevins and Iwan (1974), Robertson et al. (2003), Luongo et al. (2007), Gjelstrup and Georgakis (2011). It appears to be the only way to allow for the torsional velocity in a quasi-steady analysis, other than assuming that the forces due to the torsional velocity are zero. Having adopted quasi-steady theory and having made the assumption of the existence of an aerodynamic centre, it follows logically that the 3×3 aerodynamic damping matrix is singular (Section 2), leading to this special rotation about this point with no associated aerodynamic damping. Clearly experimental data are required to validate this predicted outcome of the analysis.

For the non-trivial solutions, the analytical expressions for the eigenvectors are rather lengthy so only they are only presented here for the simplified case of $\alpha_0 + \theta_0 + \gamma_r = 0$, i.e. when the line AO (Fig. 1) is parallel with the wind direction, for the first condition for galloping (i.e. when $\omega = \omega_n$ and Eq. (26) applies), giving

$$\left\{ \begin{array}{c} \varepsilon(C'_D - C_L)S_{3D} \\ 2\varepsilon(C_L(C'_D - C_L) + (1/2S_{3D} - C_D)(C'_L + C_D)) \\ S_{3D}^2 - (3C_D + C'_L)S_{3D} + 2(C_D(C'_L + C_D) - C_L(C'_D - C_L)) \end{array} \right\}.$$

It is obvious that these eigenvectors (for each of the two non-zero solutions for S_{3D}) are real, which corresponds to in-phase motion of the three components, which could be represented as rigid body rotation about a certain point. For the second condition for galloping (i.e. for complex responses when Eqs. (28) and (30) apply), the eigenvectors are complex, indicating phase lags between the components.

4. Application of the proposed analytical solution

In order to show typical results of the proposed analytical solutions, a square section is employed as an example, based on the data from Norberg (1993), who conducted a series of wind tunnel tests on rectangular prisms with different aspect ratios, measuring all three aerodynamic coefficients. Fig. 3 presents the aerodynamic coefficients of the square section and also a rectangular section with aspect ratio of three, chosen here since all the relevant data are available and they exhibit distinct characteristics. The aspect ratio here is defined as the ratio of the along-wind dimension to the normal dimension for zero angle of attack.

Fig. 4 shows the plot of the non-dimensional effective aerodynamic damping coefficients, S_{3D}, against angle of attack from Eq. (27) for the square section. For both the square and rectangular sections, the distance of the aerodynamic centre A from the centre of rotation O, L_a, is taken as the conventional approximation, described by Nakamura and Mizota (1975), of half the long side of the section, with the orientation of the aerodynamic centre being taken to be in line with the wind velocity.

The proposed analytical solutions are confirmed to be exact after comparing with conventional numerical eigenvalue analysis. In Fig. 4 the thin solid line shows the trivial solution, $S_{3D} = 0$, while the thick solid and dashed lines represent the two other solutions from Eq. (27). Positive values indicate aerodynamically stable solutions and negative values unstable ones. Hence galloping occurs when any one of the solutions is negative and greater in magnitude than the non-dimensional

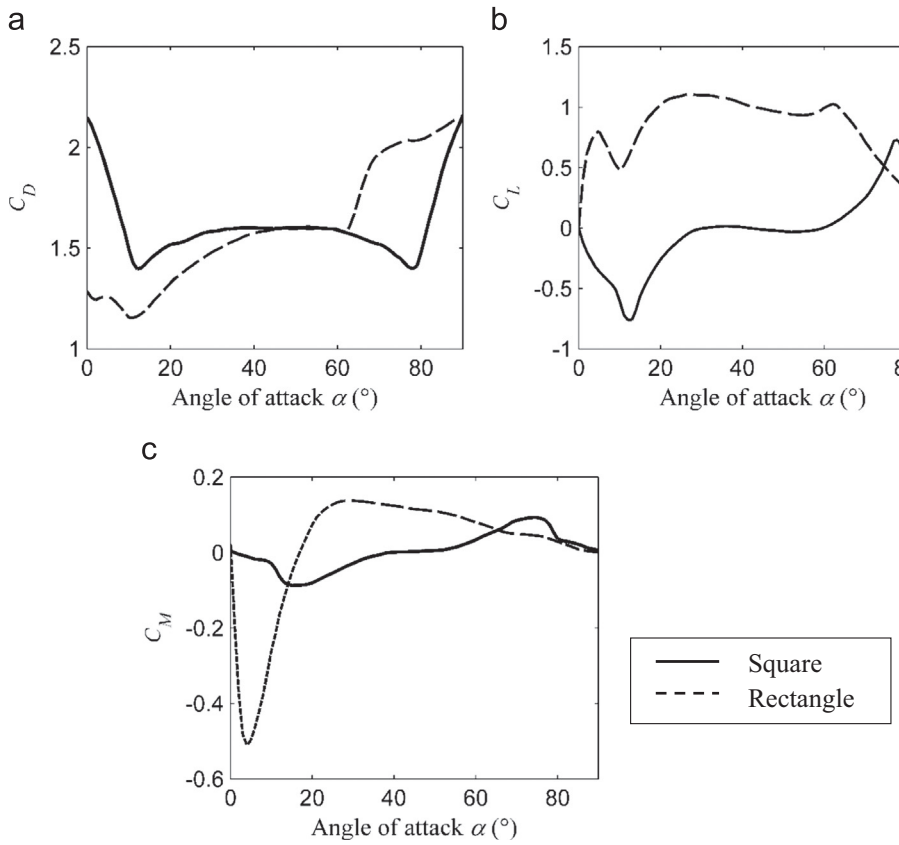

Fig. 3. Aerodynamic coefficients of the square and rectangular sections (aspect ratio 3) (Norberg, 1993): (a) drag coefficients; (b) lift coefficients; and (c) moment coefficients.

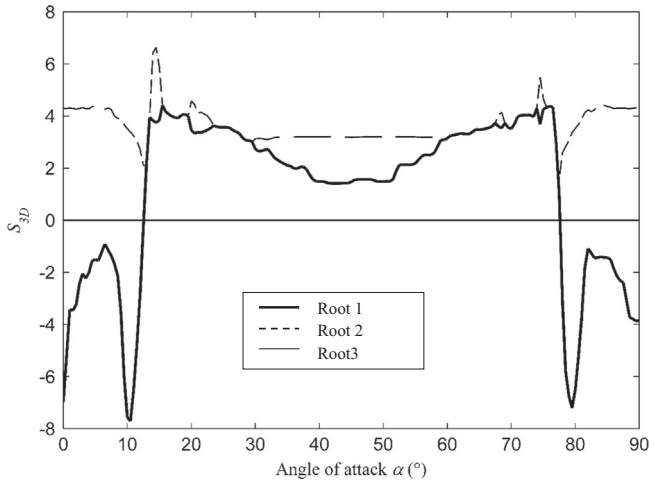

Fig. 4. Non-dimensional effective aerodynamic damping coefficient for 3DOF galloping of a perfectly tuned square section vs. angle of attack. Roots 1 and 2 are from Eq. (27) (or its real part, if complex). Root 3 is $S_{3D}=0$.

structural damping coefficient, defined as in Eq. (25) but using the actual (positive) structural damping ratio, which is the same for all three degrees of freedom ($\zeta_x=\zeta_y=\zeta_\theta$), rather than the effective aerodynamic damping ratio, ζ_a. Obviously, the solid line yields the more critical effective aerodynamic damping of the two solutions from Eq. (27). However, when the value of the solid line becomes positive, the trivial solution becomes the most critical one, although for positive structural damping is it always stable. Since the section considered is square, Fig. 4 should be symmetric about 45°. The lack of symmetry in the plot is due to slight asymmetry in the measured aerodynamic coefficients.

It can be seen that at certain angles of attack the two non-trivial solutions merge, giving a complex response, similarly to the results from Nikitas and Macdonald (2014) for 2DOF translational galloping. Although this behaviour is interesting, for the sections considered, no case has been found where it gives an aerodynamically unstable solution ($S_{3D}<0$), as for all the sections considered in the 2DOF analysis. A reason for this may be that for a complex response to occur, the expression under the square root in Eq. (27) must be negative, but since C_D is always positive the first term under the square root is likely to be large and positive unless C_L' is large and positive (noting that the translational terms tend to dominate over the torsional terms, as discussed below). However, S_{3D} is then given by the part of Eq. (27) excluding the square root which includes $3C_D+C_L'$, which under these conditions would be large and positive, tending to give a stable solution.

In order to further examine the analytical solution and also obtain a better idea of the contribution from the torsional degree of freedom, the 3DOF analytical results are compared with the 2DOF translational solution and the 1DOF torsional case, in terms of the effective aerodynamic damping coefficients. The coefficient for the 2DOF translational case with perfectly tuned natural frequencies is given by Nikitas and Macdonald (2014) as

$$S_{2D}=\frac{1}{2}\left[3C_D+C_L'\pm\sqrt{\left(C_D-C_L'\right)^2+8C_L\left(C_D'-C_L\right)}\right]. \tag{31}$$

For the 1D torsional case, the stability boundary occurs when $c_{\theta\theta}=0$, yielding an effective aerodynamic damping coefficient

$$S_{1D}=S_{\theta\theta}=\kappa\varepsilon\left(2C_M s_{\alpha\theta\gamma}+C_M' c_{\alpha\theta\gamma}\right). \tag{32}$$

For $\alpha_0+\theta_0+\gamma_r=0$, i.e. for the free stream wind direction parallel with AO in Fig. 1, this reduces to the conventional torsional galloping stability criterion given by (Blevins, 1994). Eq. (32) is a generalised expression allowing for arbitrary direction of the wind with respect to the position of the aerodynamic centre.

By inspection, it is evident that Eq. (27) reduces to Eqs. (31) and (32) when the torsional (C_M) and translational (C_D, C_L) effects, respectively, are neglected.

In addition to the aforementioned square and rectangular sections, two more sections have been considered as examples, namely an equilateral triangular section (Tatsuno et al., 1990) and a lightly iced cable (ice shape 2, using the aerodynamic coefficients measured at $U=41$ m/s, i.e. $\mathrm{Re}=1.9\times10^5$, from (Gjelstrup et al., 2012)). For the lightly iced cable, after comparing the numerical calculations with test results, Gjelstrup and Georgakis (2011) found it reasonable to take the aerodynamic centre as at the leading edge, so that has been adopted here. For the triangular section L_a has been taken to equal one third of the side length.

Fig. 5 shows the analytical results of the effective aerodynamic damping coefficients for the four shapes considered. For each shape, three scenarios are addressed: (1) pure torsional galloping (1DOF), from Eq. (32); (2) 2DOF coupled translational galloping with perfectly tuned structural natural frequencies, from Eq. (31); (3) 3DOF coupled galloping with perfectly tuned structural natural frequencies, from Eq. (27). For the 2DOF and 3DOF cases only the more critical solution of the relevant equation is given, i.e., using the negative square root (if real). A thin solid line is also plotted at $S_{3D}=0$ in each figure as a reference line indicating the aerodynamic stability boundary and the trivial solution for the 3DOF system, which is sometimes the most critical one.

The 3DOF results are generally close to those for the 2DOF translational system, but there are exceptions, most notably for the rectangular section, and often the inclusion of the torsional degree of freedom modifies the results, especially in the range of critical angles of attack. The reason for that from observation could be the torsional effective aerodynamic damping is normally significant at those angles of attack. An impression from Fig. 5 is that for most angles of attack the 3DOF curve seems to be a combination of the 2DOF one and 1DOF torsional one, reflecting the relationships between Eqs. (27), (31) and (32). The stability of the 1DOF torsional case normally makes only minor changes to the 2DOF solution to give the 3DOF solution, which agrees with Luongo et al. (2007), who claimed the torsional velocity has a negligible effect on the aerodynamic forces and thus was excluded in their subsequent analysis. However, their order-of-magnitude analysis was based on the parameters of a typical transmission line so their conclusion may not necessarily hold for other structures and cross-sections. As for example shown in Fig. 5(a), at certain angles of attack, torsion indeed has a noticeable influence on the dynamic stability of the square section. On the other hand, Fig. 5(c), in which a lightly iced cable is presented, the influence of torsion becomes relatively small for almost the whole range of angles of attack, since the cross section resembles that of a typical transmission line.

For the square section (Fig. 5(a)), the most unstable angle of attack is around 10° (or 80°) for all three cases, with the 3DOF case being significantly more unstable than the 2DOF one. For angles of attack at or close to 0° torsional galloping instability is not normally considered important since, although C_M' is negative it is very small for a square section (Blevins, 1994). However around 10° it is negative and somewhat larger (see Fig. 3(c)), leading to significant instability of 1DOF torsional galloping in this region (Fig. 5). For the worst case angle of attack the 2DOF translational system is more unstable, but for the 3DOF system these two effects are combined to make it more unstable than either system alone. The results are shown for the case of perfect tuning between all three structural degrees of freedom, for which the effects of the aerodynamic damping coupling are greatest. If the torsional degree of freedom is detuned the coupling becomes less important and the critical solution tends towards that for the 2DOF translational system. The square section is also very unstable

around 0° (or 90°), being more so for the 3DOF case than the other two. In the stable region, from around 20° to 70°, the 2DOF and 1DOF cases are stable, with the effects being combined to make the 3DOF system even more stable.

For the triangular section and lightly iced cable (Fig. 5(b) and (c), respectively) the stability of the coupled 3DOF motion follows that of the 2DOF translational case closely, with minor influence of the torsional degree of freedom. However, at some angles, mostly the critical angles of attack, where the torsional damping also tends to be relatively large, there are noticeable differences in the results. It is most significant at $\alpha=0°$ for the triangular section, where it makes the 3DOF system stable, and at the minima at 5° and 35°, where the positive torsional damping reduces the instability of the 3DOF system relative to the 2DOF one. Nevertheless, the 3DOF results are almost identical to the 2DOF ones at angles from 50° to 60°, where the torsional damping is much larger than 0 but loses its influence on the system.

With regard to the lightly iced cable, again it is at the most critical angles of attack that the torsional degree of freedom has most influence on the results. In this case, at -30° and +35° the 2DOF effective aerodynamic damping is a minimum, but it also is for the 1DOF torsional system, which slightly increases the instability for the 3DOF system at these two angles. However, at angles −65° to −80° and +65° to +85°, the torsional aerodynamic damping is obviously greater than zero but it makes little difference in the overall stability of the 3DOF system. Unfortunately, there appears to be no available experimental data of any perfectly tuned system in the literature for direct comparison with the results of the present analysis. For the lightly iced cable the dynamic experiments by Gjelstrup et al. (2012) only allow for cross-wind motion and torsion with large frequency detuning. However, a numerical analysis employing the full aerodynamic damping matrix (Eq. (11)) and the appropriate structural parameters was conducted, which gave excellent agreement with the stability predictions in that paper (which used the Routh-Hurwitz criterion), as expected.

Although the quasi-steady theory may not be very applicable for rectangular sections with large aspect ratio (Blevins, 1994; Païdoussis et al., 2010), it is still interesting to examine the theoretical effect of the torsional degree of freedom on the galloping behaviour. As can be seen in Fig. 5(d), the behaviour of the 3:1 rectangular section is quite different from the square. For angles of attack less than 10° the torsional stability has a major effect on the stability of the 3DOF system. While

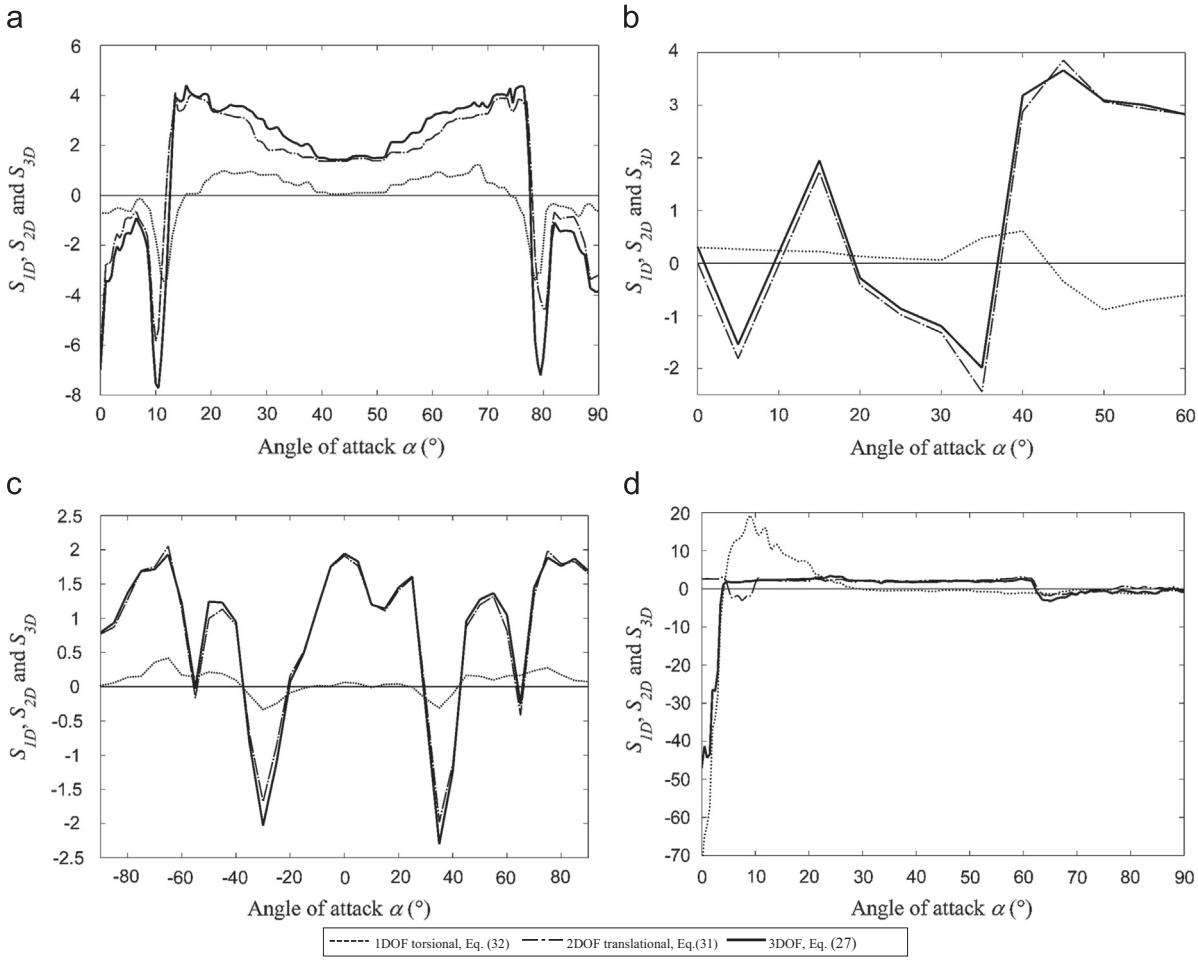

Fig. 5. Comparison between 3DOF solution and other results: (a) square section; (b) equilateral triangular section; (c) lightly iced cable; and (d) rectangular section (aspect ratio=3).

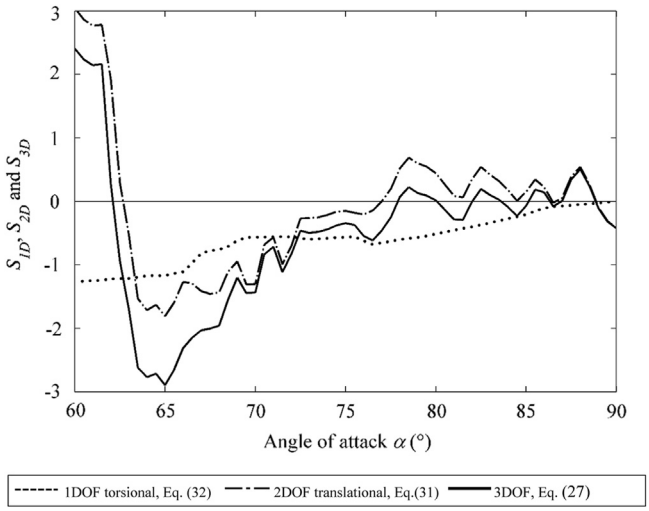

Fig. 6. Comparison between analytical solutions for a rectangular section at high angles of attack.

the 2DOF translational motion is predicted to be stable close to $\alpha=0°$, it is very unstable for pure torsion and for the 3DOF case.

For translational galloping, the square and rectangular sections clearly show dissimilar unstable ranges of angles of attack, which is consistent with the findings of Robertson et al. (2003). It may be noted that their computational simulations were conducted at low Reynolds numbers, which may not be representative of galloping of structures in the field. However, for the present analysis, the actual Reynolds number may not be so important, since the aerodynamics of sharp-cornered sections are generally insensitive to it. In contrast, the reduced velocity is generally considered to be more important in the application of quasi-steady theory. In their cases, the reduced velocity was 40 for torsional galloping and up to 80 for translational galloping, which would generally be considered to be sufficiently high. As to their findings, their 3DOF computational simulations reveal the occurrence of large-amplitude translational galloping at zero incidence for sections with aspect ratio <2 (c.f. negative S_{2D} in Fig. 5(a) for the square section at $\alpha=0°$) and negligible oscillation for sections with larger aspect ratio (c.f. positive S_{2D} in Fig. 5(d) for the rectangular section at $\alpha=0°$). This also concurs with experimental work by Washizu et al. (1978), who observed no translational galloping for rectangular sections with aspect ratio >2.5. The difference in the behaviour may be explained by flow reattachment being fully achieved for rectangular sections with aspect ratio larger than 2, as found in numerical simulations of the flow by Sohankar et al. (1997). As to the pure rotational stability, Robertson et al. (2003) numerically found severe galloping instability for square and any rectangular sections with negative C'_M at 0° angle of attack, as also reported from previous experiments (Blevins, 1994; Luo et al., 1998; Nakamura and Mizota, 1975). Hence, the analytical solutions presented here for 1DOF torsional and 2DOF translational galloping qualitatively agree well with previous numerical and experimental work.

For the rectangular section, as the angle of attack approaches 90° the aspect ratio becomes 1:3, which means quasi-steady theory is likely to be more applicable (Blevins, 1994). For this angle range the results from Fig. 5(d) are shown on an expanded scale in Fig. 6. It is clear that torsion is of importance in affecting the stability of the 3DOF system. The curve for the 3DOF solution again shares a similar pattern as that for the 2DOF solution but the system is significantly less stable due to the instability of the torsional degree of freedom.

5. Conclusions

In this paper, the full aerodynamic damping matrix has been derived, based on quasi-steady theory, for a general two-dimensional rigid cross-section with 3 degrees of freedom (heave, sway and torsion), for arbitrary orientation of the wind direction relative to the structural principal axes. An analytical solution has then been obtained for the galloping stability of a perfectly tuned 3DOF system with any aerodynamic damping matrix (i.e. not necessarily derived from quasi-steady theory). Using the property of the 3DOF quasi-steady aerodynamic damping matrix that its determinant is always zero, the solution simplifies and a closed-form expression has been found for the effective aerodynamic damping coefficient for galloping of the 3DOF system, for the first time. This has been validated against the results of conventional numerical eigenvalue analysis.

For further insight on 3DOF galloping instability, square, rectangular, equilateral triangular sections and a lightly iced cable have been employed as examples to identify the effects of incorporating the torsional degree of freedom, through comparing the effective damping coefficient of the 3DOF model with the previous 2DOF perfectly tuned translational one (Nikitas and Macdonald, 2014) and also the pure rotational one (Blevins, 1994). It has been found that the 3DOF solution is

normally close to the 2DOF translational one but with some influence of the stability of the torsional case in some instances, especially at the critical angles of attack. Unfortunately limited experimental data from dynamic tests are available for direct comparison with the predictions of the analysis but the results are consistent with related experimental results as far as they are available.

Acknowledgement

The first author is supported by a University of Bristol Postgraduate Research Scholarship. Dr. Nikolaos Nikitas of the University of Leeds is acknowledged for providing initial information.

Appendix A

This appendix contains the proof that when both Eqs. (24) and (29) have single real root simultaneously, the real solution of Eq. (29) equals the real part of the complex solutions of Eq. (24).

For a general cubic equation

$$ax^3+bx^2+cx+d=0, \tag{A.1}$$

the general form of the roots can be written as follows:

$$x_k=-\frac{1}{3a}\left(b+u_kC+\frac{\Delta_0}{u_kC}\right),\ k=1,2,3, \tag{A.2}$$

where $u_1=1$, $u_2=\frac{-1+i\sqrt{3}}{2}$, $u_3=\frac{-1-i\sqrt{3}}{2}$ and C is defined as

$$C=\sqrt[3]{\frac{\Delta_1+\sqrt{\Delta_1^2-4\Delta_0^3}}{2}}$$

where $\Delta_0=b^2-3ac$, $\Delta_1=2b^3-9abc+27a^2d$.

Thus, the real part of the complex solution of Eq. (24) and the real solution of Eq. (29) can be expressed as follows, respectively:

$$x_1=-\frac{1}{3a_1}\left(b_1-\frac{1}{2}\left(C_1+\frac{\Delta_{01}}{C_1}\right)\right), \tag{A.3}$$

$$x_2=-\frac{1}{3a_2}\left(b_2+C_2+\frac{\Delta_{02}}{C_2}\right), \tag{A.4}$$

where the subscript 1 and 2 means the origin of the variables, i.e. corresponding to either Eq. (24) (for subscript 1) or Eq. (29) (for subscript 2).

Substituting all corresponding values, it then can be obtained

$a_2=8a_1$, $b_2=8b_1$, $\Delta_{02}=16\Delta_{01}$, $C_2=4\overline{C}_1$,
with

$$\overline{C}_1=\sqrt[3]{\frac{-\Delta_{01}+\sqrt{\Delta_{11}^2-4\Delta_{01}^3}}{2}}.$$

Since,

$$C_1=\sqrt[3]{\frac{\Delta_{01}+\sqrt{\Delta_{11}^2-4\Delta_{01}^3}}{2}}.$$

Thus, $\overline{C}_1\cdot C_1=-\Delta_{01}$.

Substituting all the above parameters back into Eqs. (A.3) and (A.4), one can have

$$x_2=-\frac{1}{3a_1}\left(b_1+12\left(\overline{C}_1+\frac{\Delta_{01}}{\overline{C}_1}\right)\right).$$

Leading to

$$x_1-x_2=\frac{1}{2}\left(C_1+\overline{C}_1+\Delta_{01}\left(\frac{1}{C_1}+\frac{1}{\overline{C}_1}\right)\right)=\frac{1}{2}\left(C_1+\overline{C}_1+\Delta_{01}\frac{C_1+\overline{C}_1}{C_1\overline{C}_1}\right)=\frac{1}{2}\left(C_1+\overline{C}_1+\Delta_{01}\frac{C_1+\overline{C}_1}{-\Delta_{01}}\right)=0.$$

Therefore, the real solution of Eq. (29) equals the real part of the complex roots of Eq. (24).

References

Blevins, R.D., Iwan, W.D., 1974. The galloping response of a two-degree-of-freedom system. Journal of Applied Mechanics 41, 1113.

Blevins, R.D., 1994. Flow-induced Vibration. Van Nostrand Reinhold, New York.

Carassale, L., Freda, A., Piccardo, G., 2005. Aeroelastic forces on yawed circular cylinders: quasi-steady modeling and aerodynamic instability. Wind and Structures 8, 373–388.

Chabart, O., Lilien, J.L., 1998. Galloping of electrical lines in wind tunnel facilities. Journal of Wind Engineering and Industrial Aerodynamics 74–76, 967–976.

Chen, X.Z., Kareem, A., 2006. Revisiting multimode coupled bridge flutter: Some new insights. Journal of Engineering Mechanics – ASCE 132, 1115–1123.

Den Hartog, J., 1932. Transmission line vibration due to sleet. Transactions of the American Institute of Electrical Engineers 4, 1074–1076.

Gjelstrup, H., Georgakis, C.T., 2011. A quasi-steady 3 degree-of-freedom model for the determination of the onset of bluff body galloping instability. Journal of Fluids and Structures 27, 1021–1034.

Gjelstrup, H., Georgakis, C.T., Larsen, A., 2012. An evaluation of iced bridge hanger vibrations through wind tunnel testing and quasi-steady theory. Wind and Structures 15, 385–407.

Jones, K.F., 1992. Coupled vertical and horizontal galloping. Journal of Engineering Mechanics-ASCE 118, 92–107.

Li, Q.S., Fang, J.Q., Jeary, A.P., 1998. Evaluation of 2D coupled galloping oscillations of slender structures. Computers and Structures 66, 513–523.

Luo, S.C., Chew, Y.T., Lee, T.S., Yazdani, M.G., 1998. Stability to translational galloping vibration of cylinders at different mean angles of attack. Journal of Sound and Vibration 215, 1183–1194.

Luongo, A., Piccardo, G., 2005. Linear instability mechanisms for coupled translational galloping. Journal of Sound and Vibration 288, 1027–1047.

Luongo, A., Zulli, D., Piccardo, G., 2007. A linear curved-beam model for the analysis of galloping in suspended cables. Journal of Mechanics of Materials and Structures 2, 675–694.

Macdonald, J.H.G., Larose, G.L., 2006. A unified approach to aerodynamic damping and drag/lift instabilities, and its application to dry inclined cable galloping. Journal of Fluids and Structures 22, 229–252.

Macdonald, J.H.G., Larose, G.L., 2008a. Two-degree-of-freedom inclined cable galloping—Part 1: General formulation and solution for perfectly tuned system. Journal of Wind Engineering and Industrial Aerodynamics 96, 291–307.

Macdonald, J.H.G., Larose, G.L., 2008b. Two-degree-of-freedom inclined cable galloping—Part 2: analysis and prevention for arbitrary frequency ratio. Journal of Wind Engineering and Industrial Aerodynamics 96, 308–326.

Modi, V.J., Slater, J.E., 1983. Unsteady aerodynamics and vortex induced aeroelastic instability of a structural angle section. Journal of Wind Engineering and Industrial Aerodynamics 11, 321–334.

Nakamura, Y., Mizota, T., 1975. Torsional flutter of rectangular prisms. Journal of the Engineering Mechanics Division – ASCE 101, 125–142.

Nikitas, N., Macdonald, J.H.G., 2014. Misconceptions and generalizations of the Den Hartog galloping criterion. Journal of Engineering Mechanics – ASCE 140, 04013005.

Norberg, C., 1993. Flow around rectangular cylinders-pressure forces and wake frequencies. Journal of Wind Engineering and Industrial Aerodynamics 49, 187–196.

Novak, M., 1969. Aeroelastic galloping of prismatic bodies(Self excited aeroelastic galloping oscillations of long prismatic bodies subjected to wind velocity, noting effect of aerodynamically unstable cross sections). Journal of the Engineering Mechanics Division – ASCE 95, 115–142.

Païdoussis, M.P., Price, S.J., De Langre, E., 2010. Fluid–Structure Interactions: Cross-flow-induced Instabilities. Cambridge University Press.

Piccardo, G., 1993. A methodology for the study of coupled aeroelastic phenomena. Journal of Wind Engineering and Industrial Aerodynamics 48, 241–252.

Piccardo, G., Carassale, L., Freda, A., 2011. Critical conditions of galloping for inclined square cylinders. Journal of Wind Engineering and Industrial Aerodynamics 99, 748–756.

Piccardo, G., Pagnini, L., Tubino, F., 2014a. Some research perspectives in galloping phenomena: critical conditions and post-critical behavior. Continuum Mechanics and Thermodynamics, 1–25.

Piccardo, G., Tubino, F., Luongo, A., 2014b. A shear–shear torsional beam model for nonlinear aeroelastic analysis of tower buildings. Zeitschrift für angewandte Mathematik und Physik, 1–19.

Robertson, I., Li, L., Sherwin, S.J., Bearman, P.W., 2003. A numerical study of rotational and transverse galloping rectangular bodies. Journal of Fluids and Structures 17, 681–699.

Slater, J.E., 1969. Aeroelastic Instability of a Structural Angle Section (Ph.D. thesis). University of British Columbia.

Sohankar, A., Norberg, C., Davidson, L., 1997. Numerical simulation of unsteady low-Reynolds number flow around rectangular cylinders at incidence. Journal of Wind Engineering and Industrial Aerodynamics 71, 189–201.

Strømmen, E., Hjorth-Hansen, E., 1995. The buffeting wind loading of structural members at an arbitrary attitude in the flow. Journal of Wind Engineering and Industrial Aerodynamics 56, 267–290.

Tatsuno, M., Takayama, T., Amamoto, H., Ishii, K., 1990. On the stable posture of a triangular or a square cylinder about its central axis in a uniform-flow. Fluid Dynamics Research 6, 201–207.

Theodorsen, T., 1935. General Theory of Aerodynamic Instability and the Mechanism of Flutter. NACA, Langley Field, United States.

Wang, J.W., Lilien, J.L., 1998. Overhead electrical transmission line galloping-A full multi-span 3-DOF model, some applications and design recommendations. IEEE Transactions on Power Delivery 13, 909–916.

Washizu, K., Ohya, A., Otsuki, Y., Fujii, K., 1978. Aeroelastic instability of rectangular cylinders in a heaving mode. Journal of Sound and Vibration 59, 195–210.

Yu, P., Desai, Y.M., Shah, A.H., Popplewell, N., 1993a. Three-degree-of-freedom model for galloping. Part I: formulation. Journal of Engineering Mechanics – ASCE 119, 2404–2425.

Yu, P., Desai, Y.M., Popplewell, N., Shah, A.H., 1993b. Three-degree-of-freedom model for galloping. Part II: solutions. Journal of Engineering Mechanics – ASCE 119, 2426–2448.